Biosensors and Bioelectronics 62 (2014) 274–279

Contents lists available at ScienceDirect

Biosensors and Bioelectronics

journal homepage: www.elsevier.com/locate/bios

A novel electrochemical biosensor for ultrasensitive and specific detection of DNA based on molecular beacon mediated circular strand displacement and rolling circle amplification

Wei Cheng [b], Wei Zhang [a], Yurong Yan [a], Bo Shen [a], Dan Zhu [a], Pinhua Lei [a], Shijia Ding [a,*]

[a] Key Laboratory of Clinical Laboratory Diagnostics, Ministry of Education, College of Laboratory Medicine, Chongqing Medical University, Chongqing 400016, PR China

[b] The Center for Clinical Molecular Medical detection, the First Affiliated Hospital of Chongqing Medical University, Chongqing 400016, PR China

ARTICLE INFO

Article history:
Received 1 May 2014
Received in revised form
23 June 2014
Accepted 24 June 2014
Available online 1 July 2014

Keywords:
Circular isothermal strand displacement amplification
Rolling circle amplification
Alkaline phosphatase
Electrochemical DNA sensor

ABSTRACT

A novel electrochemical biosensing strategy was developed for ultrasensitive and specific detection of target DNA using a cascade signal amplification based on molecular beacon (MB) mediated circular strand displacement (CSD), rolling circle amplification (RCA), biotin–strepavidin system, and enzymatic amplification. The target DNA hybridized with the loop portion of MB probe immobilized on the gold electrode and triggered the CSD, leading to multiple biotin-tagged DNA duplex. Furthermore, via biotin–streptavidin interaction, the RCA was implemented, producing long massive tandem-repeat DNA sequences for binding numerous biotinylated detection probes. This enabled an ultrasensitive electrochemical readout by further employing the streptavidin-alkaline phosphatase. The proposed biosensor showed very high sensitivity and selectivity with a dynamic response range from 1 fM to 100 pM. The proposed strategy could have the potential for applying in clinical molecular diagnostics and environmental monitoring.

© 2014 Elsevier B.V. All rights reserved.

1. Introduction

Highly sensitive and specific detection of sequence-specific DNA plays essential roles in clinical diagnosis and therapy, pathogen detection and environmental monitoring (Li et al., 2010; Wang et al., 2011; Zhang et al., 2013; Xia et al., 2010). In recent years, various biosensors, including fluorescent (Ryoo et al., 2012), colorimetric (Zhou et al., 2013), chemiluminescent (Wang et al., 2012), and electrochemical (Gao et al., 2013; Ren et al., 2010) methodologies have been developed. Among these protocols, the electrochemical technique as a promising tool for DNA detection has attracted particular attention in different fields owing to its great advantages, such as simplicity of construction, low-cost, ease of use, small-sized commercial detector, high sensitivity and selectivity (Lei and Ju, 2012; Cash et al., 2009; Liu et al., 2005).

To explore the development of ultrasensitive electrochemical DNA sensor, a variety of amplification strategies have been reported by using amplification labels such as enzymes (Cai et al., 2013), nanomaterials (Xu et al., 2014) and electrochemical active substances (Liu et al., 2012), or by employing various DNA isothermal amplification methods, including strand displacement amplification (Hu et al., 2013), exonuclease III aided signal amplification (Luo et al., 2013), and rolling circle amplification (Wang et al., 2014). Among them, rolling circle amplification (RCA) has received particular interest due to its excellent property of signal amplification. RCA exploits the continuous amplification of a circular DNA template with linear kinetics by phi29 DNA polymerase, which yields large amounts of DNA products to significantly improve the sensitivity of DNA detection under isothermal conditions (Wang et al., 2013a, 2013b; Liu et al., 1996; Ji et al., 2012). Although RCA is widely applied, it is the most significant technical problem that nonspecific RCA products cannot be completely eliminated, particularly in instances where very low amounts of the template DNA are used (Brukner et al., 2005; Inoue et al., 2006). This may counteract the specificity of RCA-based signal amplification methodologies and compromise their analytical performance.

Aiming at further improving the analytical performance of RCA-based biosensing strategies for DNA detection, this work integrated RCA with another isothermal DNA amplification method, named molecular beacon (MB) mediated circular strand displacement (CSD), to design a cascade signal amplification strategy for ultrasensitive and specific detection of DNA. CSD is based on the ability of DNA polymerase to extend an oligodeoxyribonucleotide prime for direct recycling of the target DNA. CSD

* Corresponding author. Tel.: +86 23 68485688; fax: +86 23 68485786.
E-mail addresses: dingshijia@163.com, dingshijia@cqmu.edu.cn (S. Ding).

http://dx.doi.org/10.1016/j.bios.2014.06.056
0956-5663/© 2014 Elsevier B.V. All rights reserved.

results in geometric amplification of a trace of DNA and has become an essential step for nucleic acid strand detection and quantification (He et al., 2010; Zhou et al., 2011; Dong et al., 2012). The MB mediated CSD process can transfer the conformational change of the MB into the cyclic nucleic acid strand displacement polymerization due to the DNA recognition event. The hairpin structure of MB is beneficial for binding DNA targets efficiently and is excellent specificity for discriminating from mismatched sequence (Tsourkas et al., 2003; Bonnet et al., 1999).

In this study, a novel electrochemical DNA sensor was developed by combining MB mediated CSD, RCA, biotin–strepavidin system, and enzymatic amplification. The inherent properties of excellent specificity of MB mediated target binding and significant signal amplification of CSD and RCA would ensure ultrasensitivity and high specifity of the designed biosensing strategy. The proposed strategy exhibits excellent analytical performance towards DNA detection, which might provide a promising sensing platform for bioanalysis, clinical molecular diagnostics and environmental monitoring.

2. Materials and methods

2.1. Materials and reagents

Klenow fragment (3′→5′exo$^-$) (KF exo$^-$), 10× KF buffer (500 mM Tris–HCl, 50 mM $MgCl_2$, 10 mM DTT, pH 8.0), phi29 DNA Polymerase, and 10× phi29 buffer (330 mM Tris-acetate, 100 mM Mg-acetate, 660 mM K-acetate, 1% (v/v) Tween 20, 10 mM DTT, pH 7.9) were obtained from Fermentas (Lithuania). 6-Mercapto-1-hexanol (MCH), α-naphthyl phosphate (α-NP), streptavidin-alkaline phosphatase (ST-ALP), and polyethylene glycol sorbitan monolaurate (Tween-20) were purchased from Sigma Aldrich (USA). T4 DNA Ligase, 10× T4 DNA Ligase buffer (660 mM Tris–HCl, 66 mM $MgCl_2$, 100 mM DTT, 1 mM ATP, pH 7.6), gold-view, DL20 DNA Marker and the deoxynucleotide solution mixture (dNTPs) were purchased from Takara (China). Ultrapure water obtained from a Millipore water purification system (18 MΩ, Milli-Q, Millipore) was used in all assays. All other reagents were of analytical grade.

DNA hybridization buffer was phosphate buffered saline (PBS, 137 mM NaCl, 2.5 mM Mg^{2+}, 10 mM Na_2HPO_4, 2.0 mM KH_2PO_4, pH 7.4). DNA was stored in Tris–HCl (10 mM, pH 8.0) containing 1 mM ethylenediaminetetraacetic acid. The washing buffer was PBS (0.1 M, pH 7.4) containing 0.05% (w/v) Tween-20. The DNA oligonucleotides of CSD were obtained according to the literature (Gao et al., 2013). And all oligonucleotides were synthesized by Sangon Inc. (China) and purified using high-performance liquid chromatography. The detail base sequences were described below:

Target DNA: 5′ GAA CAG CCA CCG AAC 3′.
SH-modified molecular beacon (MB): 5′ SH-$(CH_2)_6$-ATC GAT TAC CGC GTT CGG TGG CTG TTC TAC GTA ATC GAT 3′.
Biotin-modified primer (B-primer): 5′ Biotin-$(CH_2)_6$-AAA AAA AAA ATC GAT TAC 3′.
Biotinylated circular primer: 5′ Biotin-$(CH_2)_6$-AAA AAA AAA AAA CAG GGC TGG GCA TAG AAG TCA GGG CAG A 3′.
Circular template: 5′ P-TAT GCC CAG CCC TGT AAG ATG AAG ATA GCG CAG AAT GGT CGG ATT CTC AAC TCG TAT CTG CCC TGA CTT C 3′.
Detection probe: 5′ Biotin-$(CH_2)_6$-AAA AAA GCG CAG AAT GGT 3′.
Single base mismatched DNA (sDNA): 5′ GAA CAG CTA CCG AAC 3′.
Non-complementary DNA (nDNA): 5′ TGC ATC GGC AAC CCA 3′.

2.2. Apparatus

All electrochemical measurements were performed on a CHI660D electrochemical workstation (Shanghai Chenhua Instruments Co. Ltd., China) with a conventional three-electrode system composed of platinum wire as auxiliary, Ag/AgCl electrode as reference, and a 3-mm diameter gold electrode (GE) as working electrode.

2.3. Preparation of circularization mixture

100 nM circular template oligonucleotide and 100 nM biotinylated circular prime oligonucleotide were mixed in 96 μL ligation buffer (66 mM Tris–HCl, 6.6 mM $MgCl_2$, 10 mM DTT, 0.1 mM ATP, pH 7.6) and incubated at 37 °C for 30 min. Then, 4 μL of T4 DNA ligase was added and incubated at 22 °C for 1 h. After ligation, T4 DNA ligase was inactivated by heating at 65 °C for 10 min. At last, the circularization mixture was stored at −20 °C.

2.4. Preparation of the MB-modified sensing electrode

The gold electrode was polished to a mirror sequentially with 0.3 μm and 0.05 μm alumina powder, followed by ultrasonic cleaning with water, ethanol and water. Then, the electrode was soaked in the piranha solution (H_2SO_4:H_2O_2=3:1) for 10 min, followed by rinsing thoroughly with ultrapure water to eliminate other substances. 10 μL 100 nM MB probe was dropped on the prepared electrode surface and incubated overnight at 4 °C. The obtained electrode was immersed into 100 μL of 1 mM MCH solution for 1 h to block nonspecific binding sites at room temperature. The electrochemical biosensor was rinsed with the washing buffer and used for following operation.

2.5. Target DNA detection protocol

Prior to use, the prepared electrochemical sensor was further washed with washing buffer. And then 10 μL target DNA at variable concentrations was dropped on the sensor surface, incubated for 1 h at 37 °C and rinsed. Afterward, the MB mediated CSD was performed by adding 10 μL reaction mixture (2 U KF exo$^-$, 500 mM dNTPs, 100 nM B-prime, 1× KF buffer) on the electrode surface and incubated at 37 °C 2 h, and rinsed with the washing buffer. The electrode was then incubated with 10 μL of 100 nM streptavidin solution at 37 °C for 30 min and rinsed with the washing buffer. 10 μL circularization mixture was added to the electrode surface and incubated at 37 °C for 30 min. And then, RCA reaction was initiated by addition of 0.2 units of phi29 DNA polymerase in 100 μL reaction buffer (33 mM Tris-acetate, 10 mM Mg-acetate, 66 mM K-acetate, 0.1% (v/v) Tween 20, 1 mM DTT, pH 7.9) and continued 80 min at 37 °C. After washing, the electrode was incubated in 10 μL solution containing 1 μM detection probe at 37 °C for 1 h.

The electrode was then rinsed with diethanolamine buffer (DEA, 0.1 M diethanolamine, 1 mM $MgCl_2$, 100 mM KCl, pH 9.6). Subsequently, 10 μL of DEA buffer containing 1.25 μg/mL ST-ALP and 10 mg/mL BSA was dropped onto the sensor surface and incubated for 30 min at 37 °C. The electrochemical sensor was washed thoroughly with DEA buffer containing 0.05% Tween-20. The electrochemical DPV measurements were performed in DEA buffer containing 1 mg/mL of α-NP substrate with modulation time of 0.05 s, interval time of 0.017 s, step potential of 5 mV, modulation amplitude of 70 mV and potential scan from 0.0 to +0.5 V.

3. Results and discussion

3.1. Design of the electrochemical sensor

The designed electrochemical sensor and the principle of the cascade signal amplification strategy is shown in Fig. 1. First, the SH-modified molecular beacon probe (MB) was immobilized on the gold electrode though Au–thiol interaction. Upon the addition of the target DNA, the MB specifically recognized the target DNA and underwent a conformational change, resulting in opening the site for bio-primer hybridization. Following this, the hybridization with the bio-primer initiated polymerization of DNA strand in the presence of dNTPs and KF exo$^-$, which led to the release of the target DNA. The released target DNA repeatedly bound another MB to trigger the MB mediated CSD process, leading to multiple biotin-tagged DNA duplex for anchoring the RCA primers and circular templates on the biosensor surface through strong biotin–streptavidin interaction. In the presence the dNTPs and phi29 DNA polymerase, the RCA was initiated to produce massive long DNA molecules with multiple tandem-repeat sequences. Then a large number of detection probes were assembled on the RCA products for capturing the ST-ALP. Finally, ALP catalyzed the irreversible conversion of substrate α-NP to an electroactive product for producing an amplified electrochemical signal, which was better quantified by differential pulse voltammetry (DPV) than square wave voltammetry (SWV). Based on the cascade signal amplification strategy, an ultrasensitive electrochemical biosensor was successfully developed for ultrasensitive and highly specific detection of target DNA.

3.2. Characterization of electrode surface modification

In order to follow the stepwise biosensor assembly, the electrochemical impedance spectroscopy (EIS) and square wave voltammetry (SWV) were employed to investigate different stages of the sensor preparation. EIS measurements were carried out over the vibration frequency range from 10 kHz to 0.01 Hz at an initial potential of 0.195 V, a sample period of 2.0 s, and amplitude of 5 mV. The EIS curves obtained in 0.4 M KCl containing 0.5 mM $Fe(CN)_6^{3-/4-}$ were shown in Fig. 2 and the semicircle diameter of EIS curve equaled the electron transferring resistance (R_{et}). The bare gold electrode exhibited an almost straight line (curve a), reflecting excellent electrochemical conductivity. When the MB probe was self-assembled onto the bare electrode via Au–S bond, the R_{et} increased due to the poor conductivity of the DNA (curve b). The binding of the target DNA led to the R_{et} increased (curve c). Then, when the CSD occurred the resulting multiple double-strand DNA became rigid linear chain structure and formed a conductive pathway from the electrode surface to the $Fe(CN)_6^{3-/4-}$ (Huang et al., 2008). So the decreased R_{et} was shown in the curve d. Afterwards, upon the streptavidin binding onto the electrochemical sensor surface, the R_{et} increased remarkably (curve e). At the

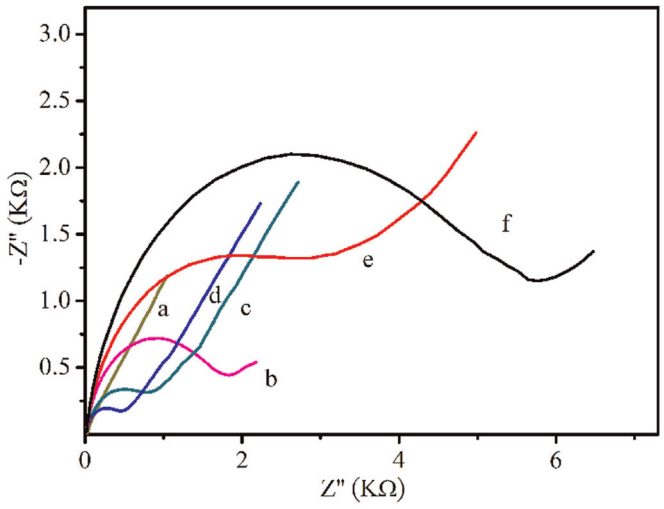

Fig. 2. EIS in 0.4 M KCl containing 0.5 mM $Fe(CN)_6^{3-/4-}$ at bare gold electrode (a), MB modified electrode (b), and MB modified electrode after hybridization with target DNA (c), CSD (d), streptavidin binding (e) and RCA (f).

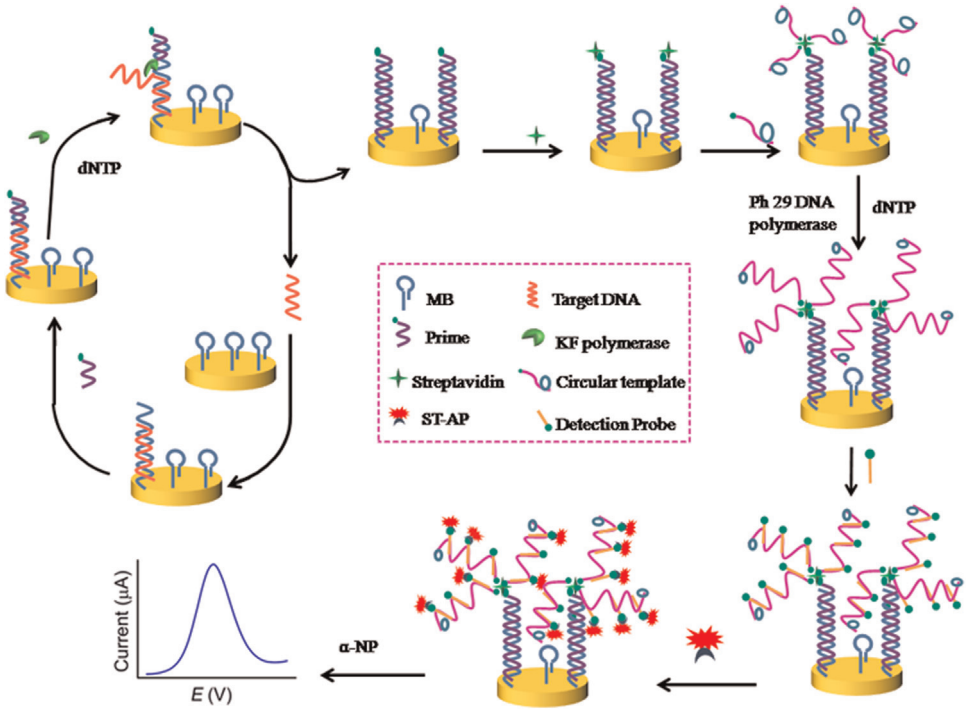

Fig. 1. Schematic illustration of the electrochemical DNA biosensor based on the cascade signal amplification of MB mediated CSD, RCA, biotin–strepavidin system, and enzymatic amplification.

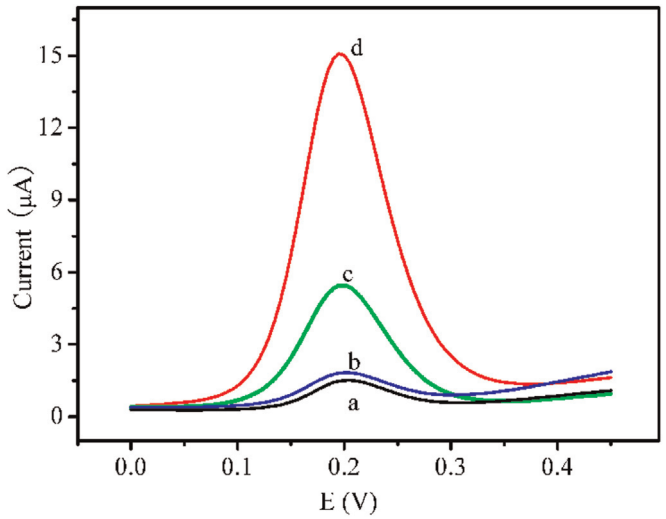

Fig. 3. Typical DPV curves of the sensor responding to blank control (a), 100 pM target DNA without (b) and with CSD (c) and CSD/RCA (d).

presence of phi29 DNA polymerase and dNTPs, RCA was triggered, producing multiple massive long DNA molecules, and resulted in R_{et} further increase (curve f). This was the direct evidence of successful processes on the developed electrochemical sensor surface. These results were in good agreement with those results obtained from SWV (data not shown), which proved the assembly, hybridization and amplification processes of the developed electrochemical sensor successful.

3.3. Verification of the cascade signal amplification strategy

To verify the feasibility of the proposed cascade signal amplification strategy for the detection of target DNA, DPV measurements were performed with or without the signal amplification strategy. As shown in Fig. 3, when the sensors were incubated without (blank, curve a) and with (curve b) 100 pM target DNA in the absence of the MB mediated CSD and RCA processes, no apparent current responses were obtained from the catalyzing reaction of ST-ALP by DPV. In the presence of the MB mediated CSD amplification, an obvious DPV response (curve c) was obtained, which was 4.5 times greater that the signal response (curve b), indicating the successful CSD and noticeable signal amplification. After implementing the RCA, the more remarkable signal amplification had been received, which demonstrated the RCA was successful (curve d).

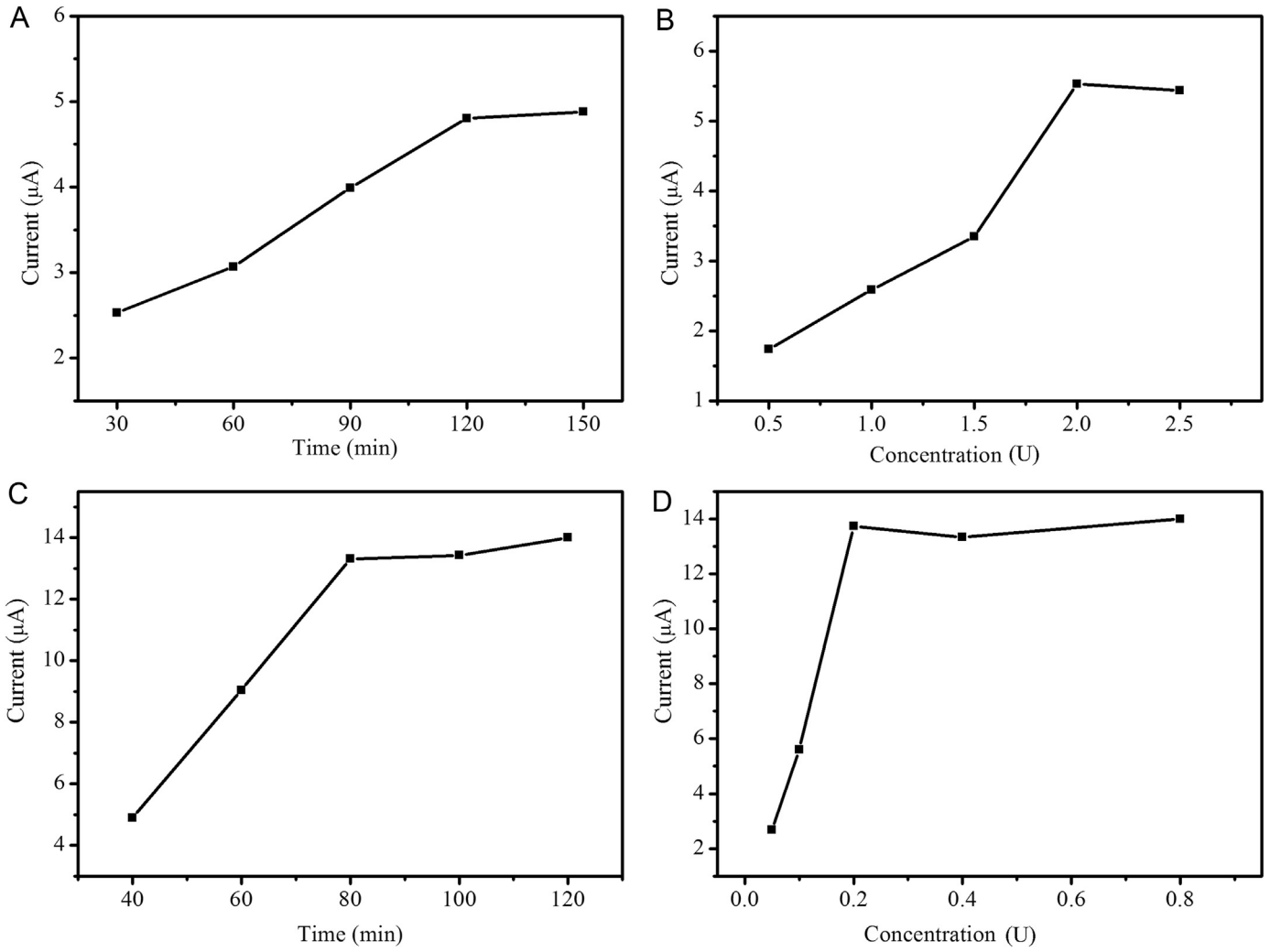

Fig. 4. Dependences of DPV peak currents on reaction time (A) and concentration of KF exo$^-$ in the CSD (B); incubating time (C) and concentration of phi29 DNA polymerase (D) in RCA. When one parameter changed the others were under their optimal conditions.

3.4. Optimization of detection conditions

To achieve optimal sensing performance, the different experimental parameters were investigated. And the peak currents of DPV were used to evaluate the performance of the proposed approach. The CSD process could be affected by the reaction time and the concentration of KF exo$^-$. The peak current increased as the increasing reaction time of the CSD from 30 min to 120 min, and then tended to a constant value (Fig. 4A). Therefore, 120 min was chosen as the optimal time and used throughout subsequent experiments. In CSD, the concentration of KF exo$^-$ was another important factor. The peak current increased until the amount of KF exo$^-$ exceeded 2 U in 10 μL CSD mixture, which was then selected as the optimal concentration (Fig. 4B).

In order to obtain higher sensitivity, the RCA experimental parameters were optimized. Fig. 4C depicts the effect of RCA incubating time on the DPV current response. As anticipated, the peak current increased rapidly with the increasing RCA reaction time, and then reached the platform at 80 min. Thus, 80 min was selected as the optimum reaction duration for RCA. The phi29 DNA polymerase in the 100 μL RCA solution was examined from 0.05 to 0.8 U (Fig. 4D). After 0.2 U the signal reached a plateau, so 0.2 U/100 μL was chosen as the appropriate concentration.

3.5. The dynamic range and sensitivity of the designed method

Under the optimal experimental conditions, the dynamic range and sensitivity of the proposed sensor was confirmed. As shown in Fig. 5A, the DPV current response gradually increased with the elevated concentration of the target DNA. The plot of the response vs. the logarithm of target DNA concentration showed a strong linear relationship in the range from 1 fM to 100 pM with a correlation coefficient of 0.993 (Fig. 5B). The error bars represented the standard deviations in three different measurements for each concentration. And the LOD was calculated to be 0.9 fM. In other words, the designed method was able to detect 0.9 zmol of target DNA in a 1 μL sample solution, which was much lower than previously reported assays (Table 1). The ultrasensitivity was attributed to the cascade signal amplification of MB mediated CSD, RCA, biotin–strepavidin system, and enzymatic amplification.

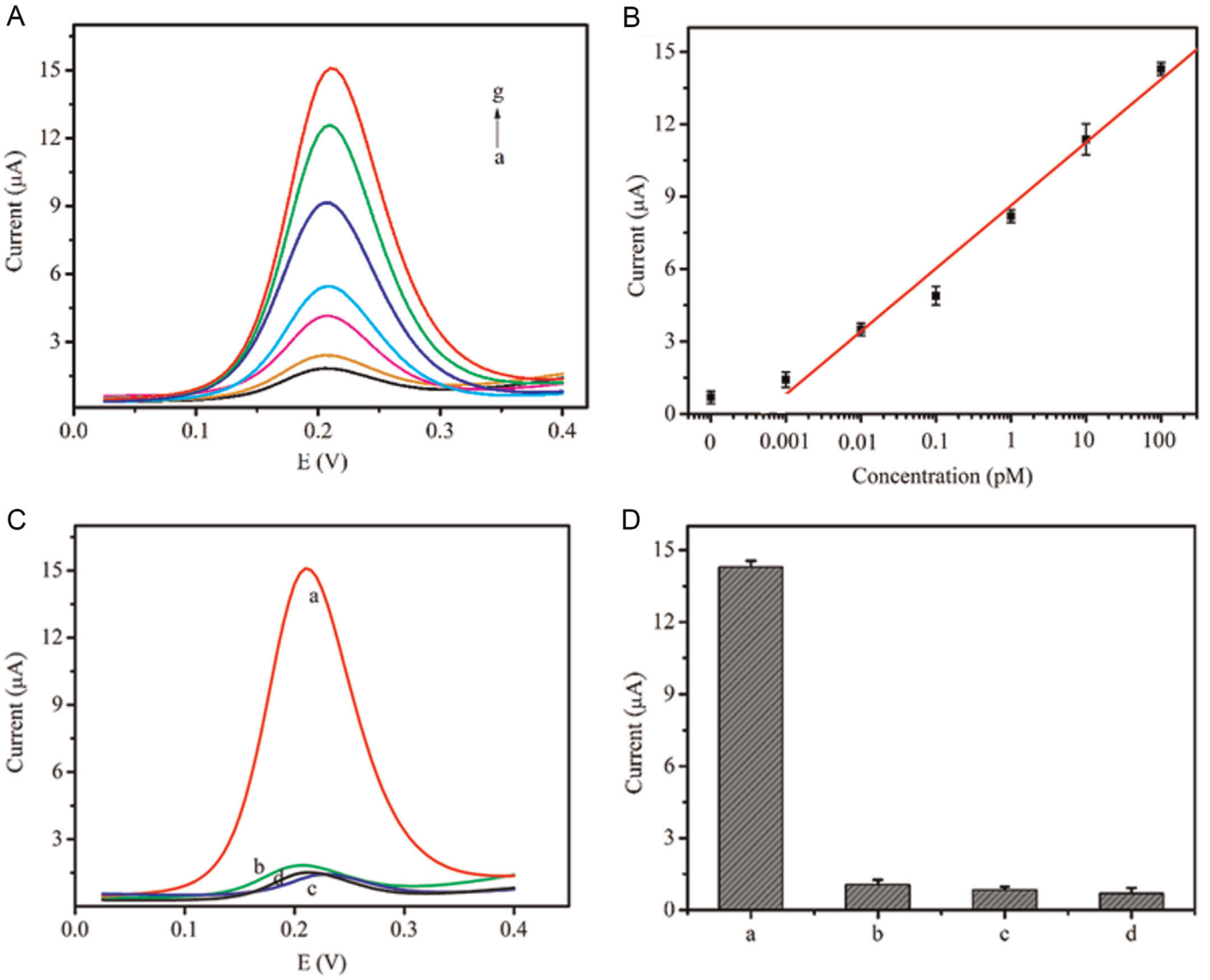

Fig. 5. (A) Typical DPV curves responding to 0, 0.001, 0.01, 0.1, 1, 10 and 100 pM of target DNA (from a to g). (B) Plot of DPV peak current vs. logarithm of target DNA concentration. (C) Typical DPV curves and (D) DPV peak currents responding to 100 pM of target DNA (a), 500 pM of sDNA (b), 500 pM of nDNA (c) and blank (d). The error bars represent the standard deviations in three different measurements for each concentration.

Table 1
Comparison between the proposed assay and other reported methods for DNA detection.

Signal amplification method[a]	Analytical technique[b]	Linear range (mol L^{-1})	Detection limit (mol L^{-1})	References
HCR	Fluorescence	5×10^{-7}–2×10^{-13}	10^{-15}	Huang et al. (2011)
CSDPR/HCR	DPV	10^{-9}–10^{-14}	8×10^{-15}	Wang et al. (2013)
CSRP/MNPs	Raman	10^{-8}–10^{-12}	4.8×10^{-13}	Gao et al. (2012)
Exonuclease	Impedance	10^{-8}–10^{-10}	4.2×10^{-11}	Xu et al. (2012)
RCA	ECL	10^{-9}–10^{-15}	10^{-15}	Jiang et al. (2014)
MB-mediated CSD/RCA	DPV	10^{-9}–10^{-15}	9×10^{-16}	This work

[a] HCR, Hybridization chain reaction; CSDPR, Circular strand-displacement polymerase reaction; CSRP, Circular strand-replacement polymerization; MNP, Magnetic nanoparticles.
[b] ECL, Electrochemiluminescence.

3.6. Selectivity and reproducibility of the proposed sensor

The selectivity of the proposed electrochemical sensor was evaluated by detecting three different kinds of control DNA sequences, including the perfectly complementary sequence, the single-base mismatched sequence (sDNA) and the non-complementary sequence (nDNA). As shown in Fig. 5C, the current responses to 500 pM of sDNA (curve b) and 500 pM of nDNA (curve c) were small and similar to that of the blank (curve d), respectively. However, the presence of target DNA at an even 100 pM concentration resulted in a remarkable increase in the current response (curve a), which was about 20 times as much as that of sDNA and nDNA (Fig. 5D). These results demonstrated the proposed biosensor displayed very high selectivity for the target DNA detection, which proved the potential application for detection of real sample and benefited from the conformational constraint of the stem-loop of MB. That is, the presence of the stem made it thermodynamically unfavorable for the binding of the mismatched sequence to the loop (Bonnet et al., 1999). In addition, the reproducibility of the prepared biosensor was further investigated by measuring the target DNA at 10 pM and 100 fM with five replicates and the coefficients of variation for both concentrations were about 2.4% and 5.6%, respectively. These results indicated good fabrication reproducibility. These results demonstrated that the electrochemical sensor was able to detect effectively the target DNA with high selectivity and reproducibility, and had great potential for clinical analysis.

4. Conclusion

In summary, this work has demonstrated a novel electrochemical sensor for ultrasensitive and specific detection of target DNA by taking the advantage of the cascade signal amplification based on MB mediated CSD, RCA, biotin–strepavidin system, and enzymatic amplification. The excellent selectivity of MB for discriminating from mismatched sequence ensures the specificity of the cascade signal amplification strategy. The designed strategy shows a broad dynamic range, ultrasensitivity, excellent specificity and good reproducibility, and does not require thermal cycling and complicated amplification labels. The proposed electrochemical sensor would provide a potential platform for DNA detection in the area of clinical diagnosis and therapy, pathogen detection and environmental monitoring in the future.

Acknowledgments

This work was funded by the National Natural Science Foundation of China (81101638 and 21075141), Natural Science Foundation Project of CQ CSTC (2012jjAl0008, 2012jjA10030 and 2013jjB10019) and the Science and Technology Plan Project of Yuzhong District of Chongqing (20120212).

References

Bonnet, G., Tyagi, S., Libchaber, A., Kramer, F.R., 1999. Proc. Natl. Acad. Sci. 96, 6171–6176.
Brukner, I., Paquin, B., Belouchi, M., Labuda, D., Krajinovic, M., 2005. Anal. Chem. 339, 345–347.
Cai, Z.M., Song, Y.L., Wu, Y.F., Zhu, Z., Yang, James, C.Y., Chen, X., 2013. Biosens. Bioelectron. 41, 783–788.
Cash, K.J., Heeger, A.J., Plaxco, K.W., Xiao, Y., 2009. Anal. Chem. 81, 656–661.
Dong, H.F., Zhang, J., Ju, H.X., Lu, H.T., Wang, S.Y., Jin, S., Hao, K.H., Du, H.W., Zhang, X.J., 2012. Anal. Chem. 84, 4587–4593.
Gao, F.L., Zhu, Z., Lei, J.P., Geng, Y., Ju, H.X., 2013. Biosens. Bioelectron. 39, 199–203.
Gao, F.L., Zhu, Z., Lei, J.P., Ju, H.X., 2012. Chem. Commun. 48, 10603–10605.
He, J.L., Wu, Z.S., Zhou, H., Wang, H.Q., Jiang, J.H., Shen, G.L., Yu., R.Q., 2010. Anal. Chem. 82, 1358–1364.
Hu, L.H., Tan, T.T., Chen, G., Zhang, K., Zhu, J.J., 2013. Electrochemical Communications 35, 104–107.
Huang, J., Wu, Y.R., Chen, Y., Zhu, Z., Yang, X.H., Yang, C.Y.J., Wang, K.M., Tan, W.H., 2011. Angew. Chem. Int. Ed. 50, 401–404.
Huang, Y.C., Ge, B.X., Sen, D., Yu, H.Z., 2008. J. Am. Chem. Soc. 130, 8023–8029.
Inoue, J., Shigemori, Y., Mikawa, T., 2006. Nucleic Acid Res. 34, e69.
Ji, H.X., Yan, F., Lei, J.P., Ju, H.X., 2012. Analyt. Chem. 84, 7166–7171.
Jiang, D.N., Liu, F., Liu, C., Liu, L.L., Li, Y., Pu, X.Y., 2014. Anal. Methods 6, 1558–1562.
Lei, J.P., Ju, H.X., 2012. Chem. Soc. Rev. 41, 2122–2134.
Li, D., Song, S.P., Fan, C.H., 2010. Acc. Chem. Res. 43, 631–641.
Liu, D.Y., Daubendiek, S.L., Zillman, M.A., Ryan, K., Kool, E.T., 1996. J. Am. Chem. Soc. 118, 1587–1594.
Liu, G., Lee, T.M.H., Wang, J., 2005. J. Am. Chem. Soc. 127, 38–39.
Liu, M.Q., Luo, C.H., Peng, H., 2012. Talanta 88, 216–221.
Luo, C.H., Tang, H., Cheng, W., Yan, L., Zhang, D.C., Ju, H.X., Ding, S.J., 2013. Biosens. Bioelectron. 48, 132–137.
Ren, R., Leng, C.C., Zhang, S.S., 2010. Chem. Commun. 46, 5758–5760.
Ryoo, S.R., Jang, H., Kim, K.S., Lee, B., Kim, K.B., Kim, Y.K., Yeo, W.S., Lee, Y., Kim, D.E., Min, D.H., 2012. Biomaterials 33, 2754–2761.
Tsourkas, A., Behlke, M.A., Rose, S.D., Bao, G., 2003. Nucleic Acids Res. 31, 1319–1330.
Wang, C., Zhou, H., Zhu, W.P., Li, H.B., Jiang, J.H., Shen, G.L., Yu, R.Q., 2013a. Biosens. Bioelectron. 47, 324–328.
Wang, D.C., Hu, L.H., Zhou, H.M., Abdel-Halim, E.S., Zhu, J.J., 2013b. Electrochem. Commun. 33, 80–83.
Wang, F., Elbaz, J., Orbach, R., Magen, N., Willner, I., 2011. J. Am. Chem. Soc. 133, 17149–17151.
Wang, F., Ma, C., Zeng, X., Li, C.Y., Deng, Y., He, N.Y., 2012. J. Biomed. Nanotechnol. 5, 786–790.
Wang, Q., Yang, C.Y., Xiang, Y., Yuan, R., Chai, Y.Q., 2014. Biosens. Bioelectron. 55, 266–271.
Xia, F., White, R.J., Zuo, X.L., Patterson, A., Xiao, Y., Kang, D., Gong, X., Plaxco, K.W., Heege, A.J., 2010. J. Am. Chem. Soc. 132, 14346–14348.
Xu, H.F., Wang, L.L., Ye, H.Z., Yu, L.S., Zhu, X., Lin, Z.Y., Wu, G.W., Li, X.H., Liu, X.X., Chen, G.N., 2012. Chem. Commun. 48, 6390–6392.
Xu, J., Wang, Q., Xiang, Y., Yuan, R., Chai, Y.Q., 2014. Analyst 139, 128–132.
Zhou, H., Liu, J., Xu, J.J., Chen, H.Y., 2011. Chem. Commun. 47, 8358–8360.
Zhang, W., Luo, C.H., Zhong, L., Nie, S.C., Cheng, W., Zhao, D., Ding, S.J., 2013. Microchim. Acta 180, 1233–1240.
Zhou, Z.X., Wei, W., Zhang, Y.J., Liu, S.Q., 2013. J. Mater. Chem. B 1, 2851–2858.